

Stationary States of a Rotating Bose-Einstein Condensate: Routes to Vortex Nucleation

K. W. Madison, F. Chevy, V. Bretin, and J. Dalibard

Laboratoire Kastler Brossel, Département de Physique de l'Ecole Normale Supérieure, 24 rue Lhomond, 75005 Paris, France*
(Received 2 January 2001)

Using a focused laser beam we stir a ^{87}Rb Bose-Einstein condensate confined in a magnetic trap. We observe that the steady states of the condensate correspond to an elliptic cloud, stationary in the rotating frame. These steady states depend nonlinearly on the stirring parameters (amplitude and frequency), and various solutions can be reached experimentally depending on the path followed in this parameter space. These states can be dynamically unstable and we observe that such instabilities lead to vortex nucleation in the condensate.

DOI: 10.1103/PhysRevLett.86.4443

PACS numbers: 03.75.Fi, 32.80.Lg, 67.40.Db

Superfluidity, originally discovered and studied in the context of superconductors and later in the system of superfluid liquid helium, is a hallmark property of interacting quantum fluids and encompasses a whole class of fundamental phenomena [1,2]. With the achievement of Bose-Einstein condensation in atomic gases [3], it became possible to study these phenomena in an extremely dilute quantum fluid, thus helping to bridge the gap between theoretical studies, only tractable in dilute systems, and experiments. One striking consequence of superfluidity is the response of a quantum fluid to a rotating perturbation. In contrast to a normal fluid, which at thermal equilibrium will rotate as a solid body with the perturbation, the thermodynamically stable state of a superfluid involves no circulation, unless the frequency of the perturbation is larger than some critical frequency, analogous to the critical velocity [1]. Moreover, when the superfluid does circulate, it can do so only by forming vortices in which the condensate density vanishes and for which the velocity field flow evaluated around a closed contour is quantized.

In this Letter we present the study of the response of a Bose-Einstein condensate (BEC) confined in a magnetic trap to a rotating perturbation created by a stirring laser beam. We observe that for a given perturbation amplitude and frequency the steady state of the condensate corresponds to an elliptic cloud, stationary in the rotating frame as predicted in [4]. Depending on the path followed in the parameter space (amplitude and frequency) of the rotating perturbation, we show that two steady states can exist, corresponding to different ellipticities of the cloud. We also observe that these states possess an intrinsic dynamical instability [4,5]; moreover, we find that this instability can lead to the transformation of the elliptic state into a state of one or more vortices. The fact that vortex nucleation seems to occur only via a dynamic instability (apart from the phase printing method explored in [6]) explains why the frequency range over which vortices are generated is notably smaller than that expected from thermodynamics ([7] and references within).

A dilute, interacting Bose gas with a large number of atoms is well described at low temperature by the hydrodynamic equations for a superfluid [8]. These equations were studied in the case of a dilute BEC in a rotating harmonic trap characterized by the trap frequencies ω_X , ω_Y , and ω_z [4] (see also [9]). The axes X, Y rotate at the frequency Ω around the z axis. There exist solutions for which the BEC wave function is given by

$$\Psi = \sqrt{\rho} \exp\left(\frac{m}{\hbar} i\alpha XY\right). \quad (1)$$

The condensate density for these solutions, in the Thomas-Fermi approximation, is a paraboloid

$$\rho = \frac{\mu_e}{g} \left[1 - \left(\frac{X^2}{R_X^2} + \frac{Y^2}{R_Y^2} + \frac{z^2}{R_z^2} \right) \right], \quad (2)$$

where $g = 4\pi\hbar^2 a/m$ is the collisional coupling constant set by the s -wave scattering length ($a = 5.5$ nm for ^{87}Rb in the $|F = 2, m_F = 2\rangle$ ground state), m is the atomic mass, and μ_e is the chemical potential in the rotating frame (the density is understood to be vanishing for $\rho \leq 0$). The XY ellipticity of the paraboloid is related to the parameter α appearing in the phase of Eq. (1)

$$\alpha = \Omega \frac{R_X^2 - R_Y^2}{R_X^2 + R_Y^2}. \quad (3)$$

The value for α is determined by the parameters of the rotating perturbation according to

$$\tilde{\alpha}^3 + \tilde{\alpha}(1 - 2\tilde{\Omega}^2) + \epsilon\tilde{\Omega} = 0, \quad (4)$$

where $\tilde{\alpha} = \alpha/\bar{\omega}$, $\tilde{\Omega} = \Omega/\bar{\omega}$, $\bar{\omega} = \sqrt{(\omega_X^2 + \omega_Y^2)}/2$, and the trap deformation $\epsilon = (\omega_X^2 - \omega_Y^2)/(\omega_X^2 + \omega_Y^2)$. Equation (4) describes the nonlinear quadrupole oscillator [10], and its solutions, corresponding to the stationary rotating state (1), are plotted as lines in Figs. 1 and 2. When $\tilde{\Omega}$ varies with a fixed ϵ (Fig. 1), or when ϵ varies with a fixed $\tilde{\Omega}$ (Fig. 2), the possible values of $\tilde{\alpha}$ are located on two branches. Branch I is a monotonic function of $\tilde{\Omega}$ or ϵ , while branch II exists only for some range of the

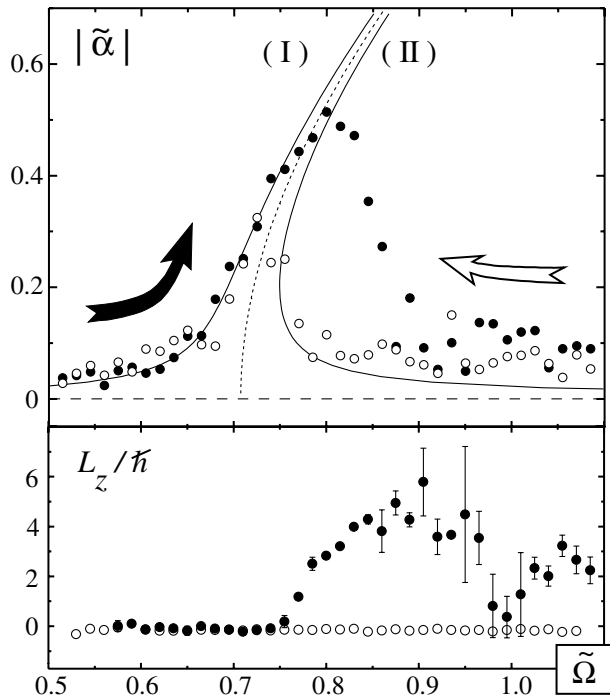


FIG. 1. Steady state value of $\tilde{\alpha}$ as a function of stirring frequency $\tilde{\Omega}$. The results of the ascending ramp are shown by a filled dot (\bullet) and of the descending ramp by a hollow dot (\circ). The branches of Eq. (4) for $\epsilon = 0$ are shown as dashed lines. The best agreement between theory and experiment was achieved for all data in Figs. 1 and 2 with $\epsilon = 0.022$ and a scaling of $\tilde{\omega}/2\pi = 200$ Hz, while the measured values are $\epsilon = 0.025 \pm 0.005$ and $\tilde{\omega}/2\pi = 195 \pm 1$ Hz. This 2% discrepancy in the frequency may be due to a deviation from the Thomas-Fermi limit. The measure of L_z after a 200 ms relaxation time reveals the presence of vortices for the ascending ramp above $\tilde{\Omega} = 0.75$.

parameters and exhibits a “backbending,” opening the possibility for hysteretic behavior.

The experimental study of these states relies on the realization of a rotating harmonic potential and a measurement of the density profile of the condensate cloud. The atoms are confined in an Ioffe-Pritchard magnetic trap which provides a static, axisymmetric harmonic potential of the form $U(\mathbf{r}) = m\omega_t^2(x^2 + y^2)/2 + m\omega_z^2z^2/2$. The condensate in this potential is cigar shaped with a length to diameter aspect ratio of $\lambda = \omega_t/\omega_z$ which was varied between 9 and 25 ($\omega_z/2\pi = 11.8 \pm 0.1$ Hz). The atomic cloud is stirred by a focused 500 μ W laser beam of wavelength 852 nm and waist $w_0 = 20$ μ m, whose position is controlled using acousto-optic deflectors [7] (see also [11]). The beam creates an optical-dipole potential which can be approximated by $m\omega_t^2(\epsilon_X X^2 + \epsilon_Y Y^2)/2$. The XY axes of the optical potential are rotated at a frequency Ω producing a rotating harmonic trap characterized by the three trap frequencies $\omega_{X,Y}^2 = \omega_t^2(1 + \epsilon_{X,Y})$ and ω_z . The transverse trap frequencies are measured directly in the rotating potential by determining the frequency domain ($\omega_Y < \Omega < \omega_X$) in which the center of mass motion of

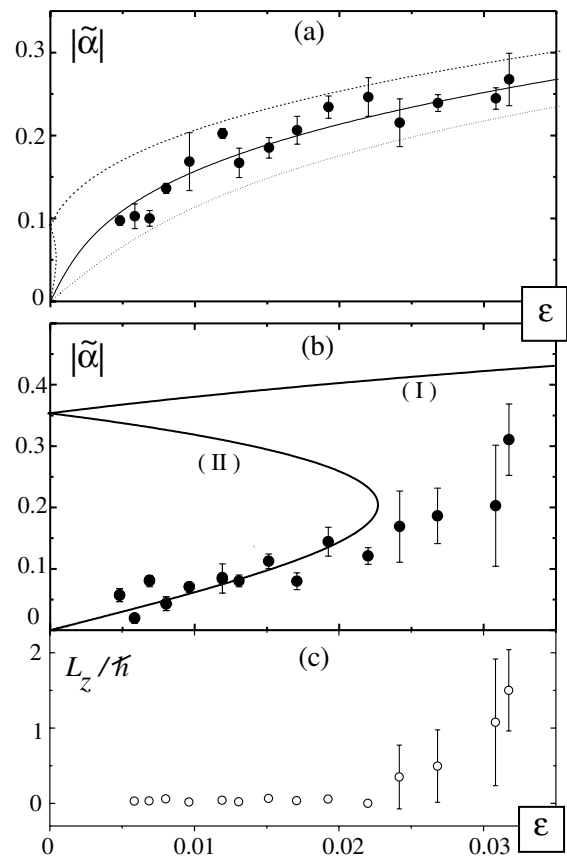


FIG. 2. Measurement of the steady state value of $\tilde{\alpha}$ obtained from a linear ramp of the stirring anisotropy for two different stirring frequencies. (a) When $\tilde{\Omega} = 0.70$ the condensate follows branch I and no vortices are nucleated. Branch I of Eq. (4) is plotted for $\tilde{\omega}/2\pi = 200$ Hz (solid line) and also for $\tilde{\omega}/2\pi = 197$ Hz and $\tilde{\omega}/2\pi = 203$ Hz (dotted and dashed lines). (b) When $\tilde{\Omega} = 0.75$ branch II is followed to the point of backbending ($\epsilon_c = 0.023$). The solid line represents the solutions of Eq. (4) for $\tilde{\omega}/2\pi = 200$ Hz. (c) For ramps which pass this point the measure of L_z after a 200 ms relaxation time reveals that vortices are nucleated.

the cloud is dynamically unstable. The steepness of this parametric instability [10] provides a precise determination of ϵ and $\tilde{\omega} = \sqrt{(\omega_X^2 + \omega_Y^2)}/2$.

To measure the density profile of the condensate we perform a field-free expansion for a duration of 25 ms, followed by a resonant absorption imaging technique along the stirring axis [12]. Using the formalism presented in [13], we have checked that after expansion the final value of α for the rotating states described by Eq. (1) differs by less than 10% from its initial value for the parameter range studied.

The experimental procedure begins with the preparation of a condensate in the pure magnetic potential by a radio-frequency (rf) evaporation ramp lasting 25 s. Starting with 10^8 atoms precooled to 10 μ K, the atomic cloud reaches the critical temperature $T_c \sim 500$ nK with an atom number of $\sim 2.5 \times 10^6$. The evaporation is continued below

T_c to a temperature of or below 100 nK at which point $3 (\pm 0.7) 10^5$ atoms are left in the condensate. The rf frequency is then set 20 kHz above $\nu_{\text{rf}}^{\text{min}}$, the rf frequency which corresponds to the bottom of the magnetic potential. This rf drive is kept present in order to hold the temperature approximately constant. At this point, the stirring laser is switched on and the condensate is allowed to evolve in the combined magnetic and optical potential for a controlled duration after which we perform the field-free expansion and optical detection.

Since the condensate is first created in a static harmonic potential and then the rotating perturbation is introduced, the final state of the condensate depends on its evolution in a time-dependent rotating potential characterized by the two parameters $\epsilon(t)$ and $\tilde{\Omega}(t)$. If the time dependencies are slow enough, the condensate at every instant is in a stationary state corresponding to the instantaneous values of ϵ and $\tilde{\Omega}$. In this case, the initial state of the condensate is $\tilde{\alpha} = 0$, and as ϵ and $\tilde{\Omega}$ evolve so does $\tilde{\alpha}$ evolve along a path defined by Eq. (4).

The first study that we performed involved switching on the optical potential with a fixed value of $\epsilon = 0.025 \pm 0.005$ and an initial frequency of $\tilde{\Omega} = 0$. The switching time (~ 20 ms) of this fixed anisotropy was long compared to $\tilde{\omega}^{-1}$ so that the excitation of collective modes of the BEC was negligible. The frequency $\tilde{\Omega}$ was increased at a constant rate to a final value in the range (0.5, 1.5) [14]. The rotation frequency was then held constant at this final value during five rotation periods, and finally the state of the condensate was measured. For each final frequency studied, two different measurements were performed: a determination of α made according to Eq. (3) and a measurement of the angular momentum per particle of the condensate (L_z) associated with the presence of a vortex. The value of L_z is determined from the precession rate of the quadrupolar oscillation resulting from the broken degeneracy of the two surface modes $m = \pm 2$ [15,16]. It is performed 200 ms after the stirring anisotropy is switched off. This delay is (i) short compared to the vortex lifetime [7] and (ii) long compared to the measured relaxation time (~ 25 ms) of the ellipticity of the rotating condensate. Hence a nonzero value of L_z is the signature of vortex nucleation. Each measurement relies on a destructive resonant-absorption imaging, and is performed independently. The results are shown in Fig. 1, together with those obtained with a descending frequency ramp starting above 1.

In both cases, the state of the condensate starts on and follows one of the branches of Eq. (4). For the descending ramp, the lower part of branch II is followed until the backbending frequency is reached below which this branch ceases to be a solution of Eq. (4). At this point, the condensate is observed to switch to branch I and to follow it down to $\tilde{\Omega} = 0$. The fact that no vortices are nucleated along this path seems to confirm the prediction that the lower part of branch II is stable [4]. For the ascending

ramp the condensate is observed to start on and to follow branch I until a frequency of $\tilde{\Omega}_c \approx 0.75$ is reached. Beyond this point the experimentally determined value of α is no longer a solution of Eq. (4), and the presence of vortices is detected in the L_z measurement. The value of $\tilde{\Omega}_c$ is in good agreement with the frequency at which branch I is expected to become dynamically unstable [5].

In the second study that we present, the stirring frequency Ω was fixed and the rotating deformation parameter ϵ was increased linearly from zero to a final value in the range (0.005, 0.032) at a constant rate $\dot{\epsilon} = 0.078 \text{ s}^{-1}$. Then, as before, we measured either $\tilde{\alpha}$ or we checked for vortex nucleation. In this case, since α is initially zero, the branch that is followed depends on which side of the rotating quadrupole resonance ($\Omega_{\text{QP}} \approx \tilde{\omega}/\sqrt{2}$) is Ω (see the dotted line in Fig. 1 corresponding to $\epsilon = 0$) [17]. The results are shown in Fig. 2, and we observe that when $\tilde{\Omega} = 0.7$ the condensate follows branch I. No vortices are nucleated in this case which is in agreement with the predicted stability of this branch [18]. By contrast, when $\tilde{\Omega} = 0.75$ the condensate follows the lower part of branch II up to a value of $\epsilon_c = 0.023$ where branch II bends backwards. Beyond this point the measured value of $\tilde{\alpha}$ is no longer a solution of Eq. (4) and we observe the nucleation of vortices. This situation is quite different from the one observed in the descending frequency ramp discussed above. In that case, when the backbending of branch II is reached no vortices are nucleated and the condensate is observed to switch to branch I.

In this second procedure, where $\tilde{\Omega}$ is fixed and ϵ increases slowly, the critical value ϵ_c at which the backbending of branch II occurs increases with increasing $\tilde{\Omega}$. This route can lead to vortex nucleation only if the final value of the ramp in ϵ is above ϵ_c , which for a given ramp, puts an upper limit on the stirring frequency leading to vortex formation. This is well confirmed experimentally; more precisely, with our maximal value of $\epsilon = 0.032$, we could nucleate vortices only when the stirring frequency was in the range $0.71 \leq \tilde{\Omega} \leq 0.77$.

A third route to vortex nucleation is followed when the rotating potential is switched on in a time τ short enough so that the adiabatic following of branch II is not possible [7,15]. This occurs when $\tau(\Omega - \Omega_{\text{QP}}) \ll 1$. In particular, for $\tau = 20$ ms, we found that vortices are nucleated along this route for $\tilde{\Omega} = 0.70$, $\epsilon = 0.032$ (final parameters in Fig. 2a) in marked contrast with the results of a slow ramp of ϵ . With this nucleation procedure, we observe that $\tilde{\alpha}$ oscillates around 0.3 during the first 200 ms, and then falls dramatically to a fixed value below 0.1 at which point we see vortices entering the condensate from the border and settling into a lattice configuration (Fig. 3). We should point out that the presence of the rotating anisotropy is not necessary beyond the first ~ 80 ms for vortex nucleation and ordering; nonetheless, the number of vortices generated is an increasing function of the stirring time after this threshold.

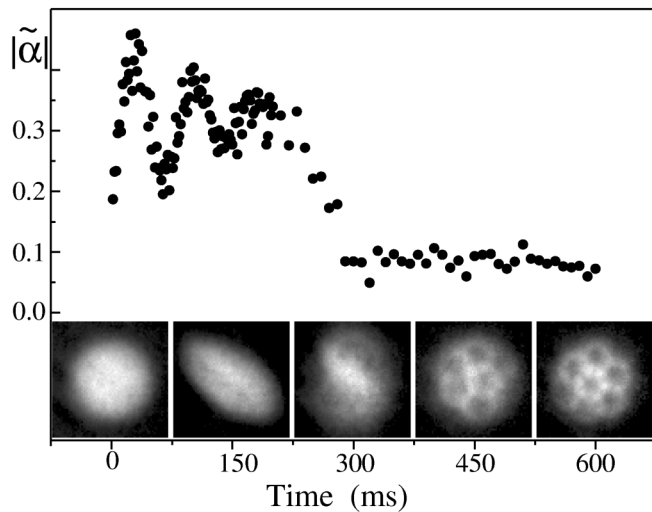


FIG. 3. Measurement of the time dependence of $\tilde{\alpha}$ when the stirring anisotropy is turned on rapidly (20 ms) to a value of $\epsilon = 0.025$ and a frequency of $\tilde{\Omega} = 0.7$ ($\lambda = 9.2$), and is held constant for 300 ms. Five images taken at intervals of 150 ms show the transverse profile of the elliptic state and reveal the nucleation and ordering of the resulting vortex lattice. The size of an image is $300 \mu\text{m}$.

In conclusion, we study the irrotational state of a condensate held in a rotating harmonic potential which corresponds to an elliptic cloud, stationary in the rotating frame. Vortex nucleation is related to dynamical instabilities of this irrotational state. This explains why the critical frequency in this system is notably larger than the one predicted by a purely thermodynamic analysis: when a vortex state is thermodynamically allowed but no dynamical instability is present, the time scale for vortex nucleation is probably too long to be observed in this system. We have obtained similar results for trap geometries λ between 9 and 25. In particular, vortex nucleation *via* the third route is always possible at a stirring frequency around Ω_{QP} over a range which increases with increasing ϵ . This independence on λ shows that the anomalous mode instability of the vortex state predicted to occur in a very elongated geometry ($\lambda > 15$) with $\tilde{\Omega} \sim 0.75$ [19] does not inhibit vortex nucleation.

A natural extension of this work is the investigation of other irrotational steady states associated with rotating potentials of higher multipole order and leading to vortex nucleation at lower stirring frequencies [11,17,20,21]. Finally, the exact role of temperature in vortex nucleation remains to be elucidated. We believe that it has conflicting roles in the generation of an ordered vortex lattice. On the

one hand, when the temperature is increased, the ellipticity induced by the stirring is reduced and vortex nucleation is hindered and may even become impossible. On the other hand, dissipation is clearly necessary to order the vortex lattice, and we observe qualitatively that the ordering time increases with decreasing temperature.

We thank the ENS Laser cooling group, G. Shlyapnikov, and S. Stringari for helpful discussions. This work is supported by CNRS, Collège de France, DRET, and DRED. K. W. M. acknowledges DEPHY for support.

*Unité de Recherche de l'Ecole normale supérieure et de l'Université Pierre et Marie Curie, associée au CNRS.

- [1] E. M. Lifshitz and L. P. Pitaevskii, *Statistical Physics, Part 2* (Butterworth-Heinemann, Stoneham, MA, 1980), Chap. III.
- [2] R. J. Donnelly, *Quantized Vortices in Helium II* (Cambridge, Cambridge, England, 1991).
- [3] For a review, see, e.g., *Bose-Einstein Condensation in Atomic Gases*, edited by M. Inguscio, S. Stringari, and C. E. Wieman (IOS Press, Amsterdam, 1999).
- [4] A. Recati *et al.*, Phys. Rev. Lett. **86**, 377 (2001).
- [5] Y. Castin and S. Sinha, cond-mat/0101292.
- [6] M. R. Matthews *et al.*, Phys. Rev. Lett. **83**, 2498 (1999).
- [7] K. W. Madison *et al.*, Phys. Rev. Lett. **84**, 806 (2000).
- [8] S. Stringari, Phys. Rev. Lett. **77**, 2360 (1996).
- [9] J. García-Ripoll and V. Pérez-Carriá, cond-mat/0003451.
- [10] L. D. Landau and E. M. Lifshitz, *Mechanics* (Mir, Moscow, 1969), Chap. 5.
- [11] R. Onofrio *et al.*, Phys. Rev. Lett. **84**, 810 (2000).
- [12] Since the typical radial size of the condensate is only $3 \mu\text{m}$, direct optical imaging is not reliable.
- [13] P. Storey and M. Olshanii, Phys. Rev. A **62**, 33 604 (2000).
- [14] The ramp lasts for 75 periods of the final frequency and so $d\Omega/dt$ never exceeds $2\pi 550 \text{ Hz/s}$. We checked that at this maximum rate the condensate follows adiabatically the branches in Fig. 1. On the other hand, the frequency ramp is fast enough so that the center of mass instability does not have enough time to develop during the time that $\tilde{\Omega}$ spends in the instability region $[1 - \epsilon/2, 1 + \epsilon/2]$.
- [15] F. Chevy *et al.*, Phys. Rev. Lett. **85**, 2223 (2000).
- [16] P. C. Haljan *et al.*, Phys. Rev. Lett. **86**, 2922 (2001).
- [17] F. Dalfovo and S. Stringari, Phys. Rev. A **63**, 011601(R) (2001).
- [18] Dynamical instability of this branch is expected for $\epsilon > 0.08$, well above the range explored experimentally [5].
- [19] D. L. Feder *et al.*, Phys. Rev. Lett. **86**, 564 (2001); A. A. Svidzinsky and A. L. Fetter, J. Phys. Condens. Matter **13**, R135 (2001).
- [20] F. Chevy *et al.*, cond-mat/0104218.
- [21] J. R. Abo-Shaer *et al.*, Science **292**, 467 (2001).